Final Technical Report
Earthquake Hazards Program Assistance Awards

USGS Award Number

G17AP00104

Title of Award

Toward Earthquake System Science: Western U.S. Lithospheric Stress/Strain Partitioning of Mantle Dynamics

Authors and Affiliations

Anthony R. Lowry
Department of Geosciences
4505 Old Main Hill
Utah State University
Logan, UT 84322-4505
Phone: +1-435-797-7096 (ofc);
+1-435-557-6780 (cel)
Fax: +1-435-797-1588
Email: tony.lowry@usu.edu

Ravi V.S. Kanda
Department of Geosciences
4505 Old Main Hill
Utah State University
Logan, UT 84322-4505

Term covered by the report

1 Sep 2017 – 31 Aug 2019

Acknowledgement of Support and Disclaimer

This material is based upon work supported by the U.S. Geological Survey under Grant No. EHP-G17AP00104. The views and conclusions contained in this document are those of the authors and should not be interpreted as representing the opinions or policies of the U.S. Geological Survey. Mention of trade names or commercial products does not constitute their endorsement by the U.S. Geological Survey.

Abstract

Physics-based investigation of seismic hazard is a grand challenge of 21st century Earth science. Recent investigations of dynamical flow predictions of lithospheric vertical stress rates demonstrate skill in predicting distributions of intraplate seismicity in the western United States, but these models are limited by a simplistic (and incorrect) representation of stress redistribution in the lithosphere. This project combined modeling to evaluate which flow modeling components are required to meaningfully simulate lithospheric stress accumulation in the real Earth with the

creation of an observation-based "real-Earth" simulation of compositional, mass density, thermal and rheological state of the U.S. lithosphere as first steps toward evaluating the roles of buoyancy-driven flow and lithospheric rheology in stress, deformation and seismicity.

Report:

Introduction

This project builds from a prior observation by Becker et al. (2015) that vertical stress rates from mantle flow are a strong predictor of western U.S. seismicity. The research for the project had three overarching goals that incrementally step toward building physics-based simulations of seismic hazard. The first goal was to evaluate how elasticity (neglected in Becker et al.'s (2015) analysis) may affect long-term evolution of membrane and bending stress in the lithosphere. A second goal was to generate improved 3D approximations of the real-Earth physical properties that are important to lithospheric dynamics– namely, mass density, mineralogy, temperature and rheology– from seismic and other data available within the USArray footprint. The third and final goal was to implement 2D and ultimately 3D dynamical flow models using the simulated real-Earth structure, for evaluation by comparing observed and modeled deformation and seismicity.

The Role of Elasticity and a Free Surface

Preliminary modeling to assess differences between viscous and elastic representations of lithospheric stress were performed by an undergraduate student, Jared Bryan, with the guidance of CoPI Kanda and PI Lowry. Although undergraduate research was not originally envisioned as a part of this project, Jared expressed interest in the problem and submitted a successful funding proposal to USU's Undergraduate Research and Creative Opportunities (URCO) program. He then implemented and examined stress in a 2D marker in cell, finite difference model of viscous flow, and compared that to behavior of a model coupled to an elastic lithosphere at the surface. Jared's analyses examined the stress response of the lithosphere with and without a free surface (simulated by a low-viscosity "sticky air" layer at the surface, after Crameri et al., 2012) and with and without elasticity of the surface layer (Fig. 1).

These modeling exercises illustrate several points that are deemed useful for analyses going forward. First, explicitly including a free surface significantly affects both stress and the vertical stress distribution (compare Figs. 1b and 1c). Secondly, implementing a rheology that maintains significant stress over geological timescales can significantly change both the stress rates and the partitioning of potential energy into strain versus density surface displacement (Figs. 1c-f). Becker et al. (2015) used a standard viscous flow model with a viscous lithosphere and no free surface. They mapped rates-of-change of vertical normal stress at the base of the lithosphere for use in Molchan analyses to evaluate skill in predicting seismicity distributions, and although they did find significant predictive skill in those stress-rate distributions, these models indicate those stress rates would be substantially different given a free surface and a more realistic lithospheric rheology. It is also worth noting that the dynamic topography predicted for a viscous lithosphere model is as much as twice that of a model with longer-term rheological strength (compare Figs. 1e and 1f). A debate has arisen in recent years regarding whether or not dynamical flow plays a significant role in surface elevation and lithospheric stress (e.g., Molnar et al., 2015), deriving partly from inferences that viscous flow models predict large dynamic elevation variations for which there is little observational support. Jared's findings suggest that this may partly stem from neglect, by viscous flow models, of the role of lithospheric strength in the minimization of potential energy that determines lithospheric stress and surface elevation. However, more accurate representation of long-term stress rates also is anticipated to require a rheological mechanism incorporating anelasticity, whether an elastic-plastic frictional rheology (e.g., Naliboff et al., 2015) or viscoelasticity (e.g., Willett et al., 1985), rather than an elastic layer. The results of Jared's modeling efforts were presented at the 2019 Utah Conference for Undergraduate Research (Bryan et al., 2019).

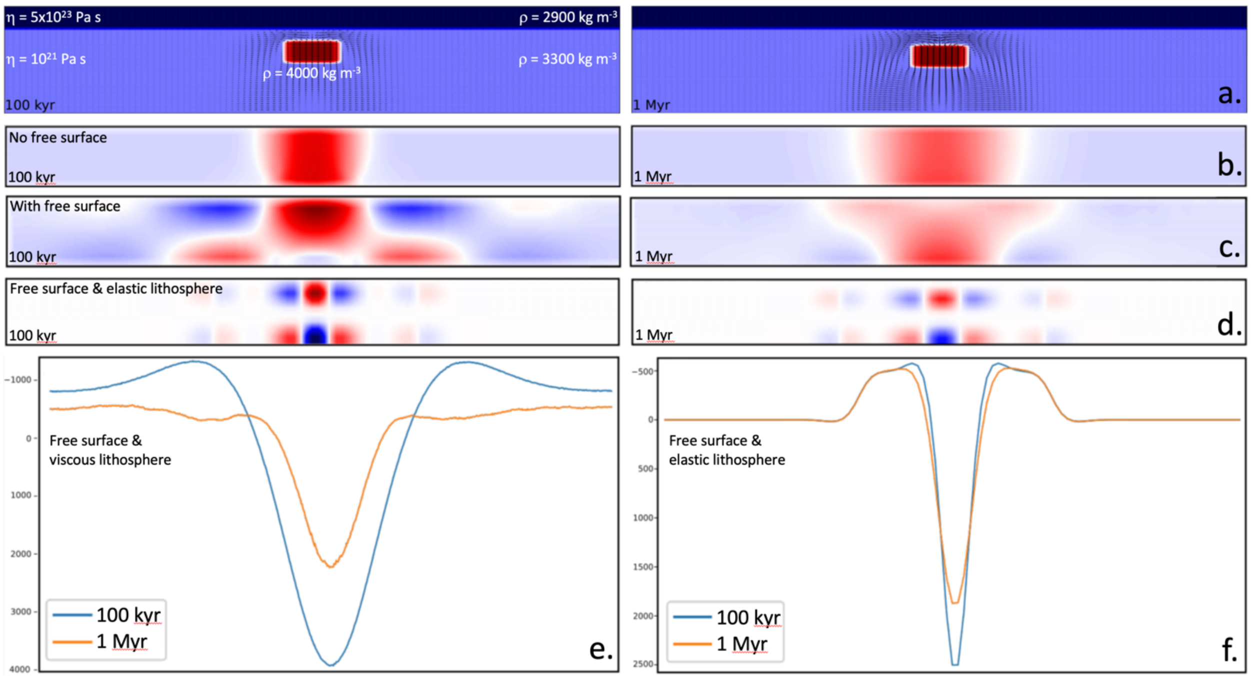

Figure 1. 2D modeling of lithospheric response to a sinking block (Bryan et al., 2019). **a,** Properties and flow of the viscous model at two time steps (100 kyr, left, and 1 Myr, right). **b,** Stress in a viscous lithosphere is compressional over the block (colorscale is $\pm 2 \times 10^8$ Pa; red/compression is positive). **c,** With a free surface, flexural stress (sign changing with depth) is evident early in the response. **d,** Flexural stress is long-lived in an elastic lithosphere. **e,** Topography of a viscous free surface is large and decays away from a flexural expression. **f,** Topography of the elastic lithosphere changes only amplitude with the change in vertical normal stress of asthenospheric flow.

A Realistic Simulated U.S. Lithosphere and Upper Mantle Asthenosphere

The development of a realistic simulation of lithospheric an upper-mantle asthenospheric properties is a crucial goal of this project. The PI Lowry generated preliminary 3D field representations of properties of temperature, mass density, and flow rheology required for dynamical modeling using a combination of USArray seismic imaging of the region (Lowry & Pérez-Gussinyé, 2011; Ma & Lowry, 2017; Buehler & Shearer, 2017; Schmandt & Lin, 2014), mineral physics (Schutt et al., 2018; Cammarano et al., 2003), and measurements of lithospheric flexural rigidity (Lowry & Pérez-Gussinyé, 2011).

The ***3D temperature*** model uses Schutt et al.'s (2018) Pn-derived estimate of Moho temperature to calculate a conductive thermal transfer model using lab thermal properties for crustal rocks and olivine. Assumed crustal heat production is consistent with standard continental crustal composition models but perturbed slightly to minimize differences between the heat flow and Pn predictions of geotherm. The geotherm in the upper crust is perturbed to more closely match Blackwell et al.'s (2007) compilation of surface heat flow, via an approach described in Ma & Lowry (2017) and developed further in Berry et al. (2021). The deep geotherm matches the Moho temperature measurement and assumes a mean adiabatic mantle reference potential temperature of 1410 °C, with perturbations to that mean derived from Schmandt & Lin's (2014) %-v_S perturbation model at 230 km using a standard mapping of v_S to temperature (Cammarano et al., 2003). A similar straight mapping of v_S to temperature is used at depths greater than 230 km to the 410 km base of the model, with no contribution from modeling of conductive thermal transfer in that depth range. A representative cross-section of model temperature at latitude 38° is shown in Fig. 2a.

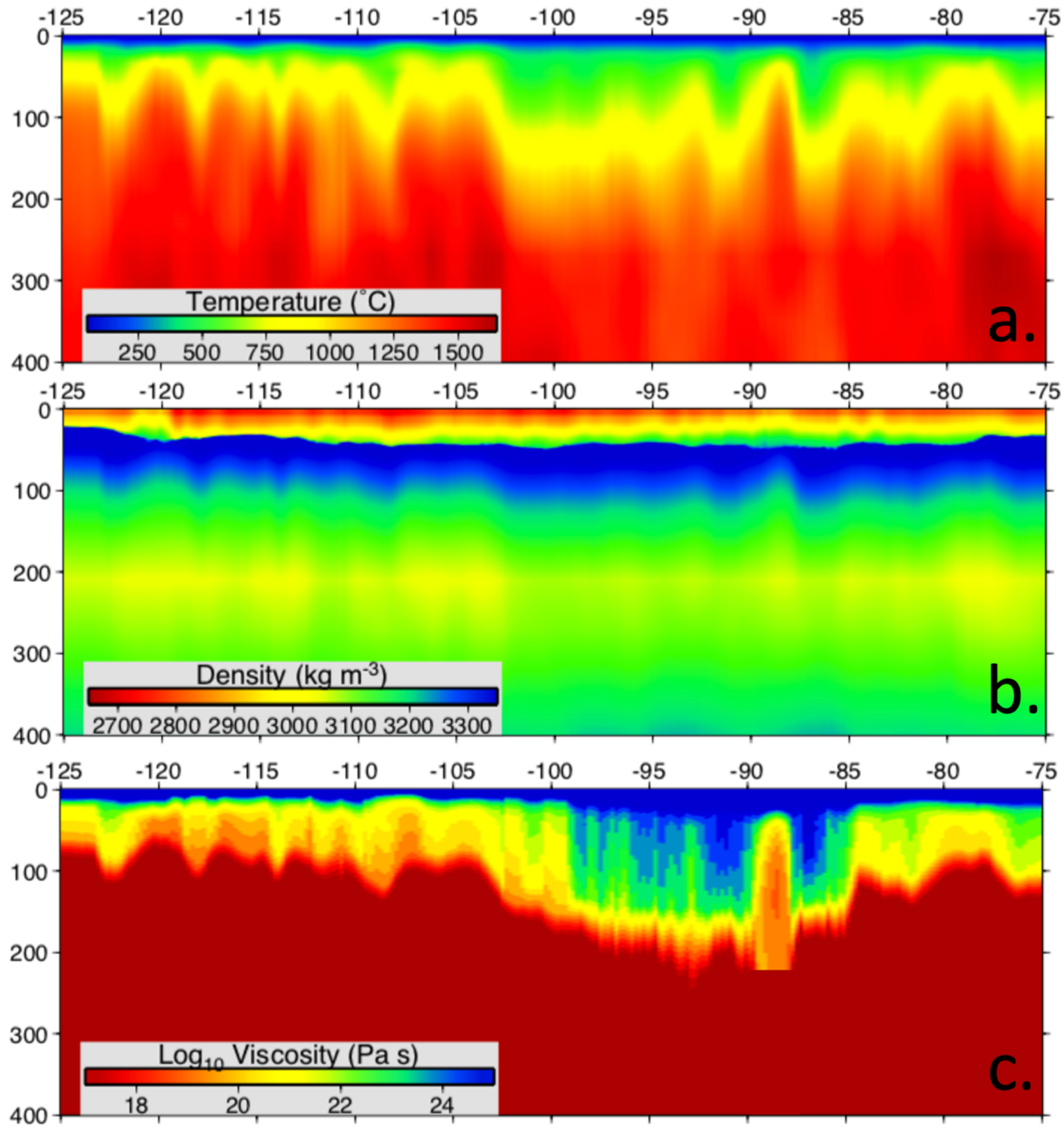

Figure 2. Representative slices through the 3D models of simulated Earth properties at 38° N; axis labels are longitude (x) versus depth (y-km). **a,** Temperature. **b,** Density. **c,** Effective viscosity.

3D density calculations assume a reference depth-dependence of continental crustal density from Christensen & Mooney (1995) and reference mantle density from AK135-F (Montagner & Kennett, 1996), adjusted slightly to match the Moho density contrast to the mean value from our joint seismic receiver function and gravity inversion calculations (Lowry & Pérez-Gussinyé, 2011; Ma & Lowry, 2017). The model was then perturbed in three dimensions to incorporate crustal thickness variations and crustal density associated with crustal v_P/v_S variations estimated from the seismic receiver function and gravity inversion. Both the crust and mantle densities also incorporate thermal density variations associated with our temperature model, using a coefficient of thermal expansion derived from the joint inversion of seismic receiver function/gravity data. A sample profile of model density is given in Fig. 2b.

3D rheology uses the receiver function/gravity model of crustal structure as a proxy for crustal-versus mantle compositional variation, assumes the temperature structure described above, and varies a water fugacity parameterization in power-law flow of the crust and mantle lithosphere to best-fit a model of lithospheric flexural rigidity to measurements. Flexural rigidity measurements derive from a new, more robust approach to isostatic modeling from coherence analysis of Bouguer gravity and topography, in which mass fields from seismic structure are incorporated as constraints on the loading structure of the lithosphere. The flexural rigidity model parameterized yield-strength envelopes using the 3D temperature product and flow law parameters derived from laboratory studies of wet- and dry olivine, feldspar and quartz compiled in Bürgmann & Dresen (2008). The mineralogical parameterization used olivine flow below the seismic Moho, quartz above the Moho when bulk-crustal $v_P/v_S \leq 1.775$ and feldspar for higher v_P/v_S (with the v_P/v_S threshold chosen from an optimization to determine which threshold best fit models to measurements). Water fugacity was permitted to vary laterally from 0 to 100% of saturation in order to minimize the misfit. The output 3D fields include a mineralogy term to indicate which flow law parameterization was used at given depth and a pre-exponential constant for effective viscosity (which incorporates a material parameter, water fugacity term and strain-rate dependence). Significant variations in hydration state are necessary to match the measured lithospheric strength variations, leading to significant perturbations to the viscosity fields that would be attributed to temperature alone (Fig. 3). A representative cross-section of effective viscosity is shown in Fig. 2c.

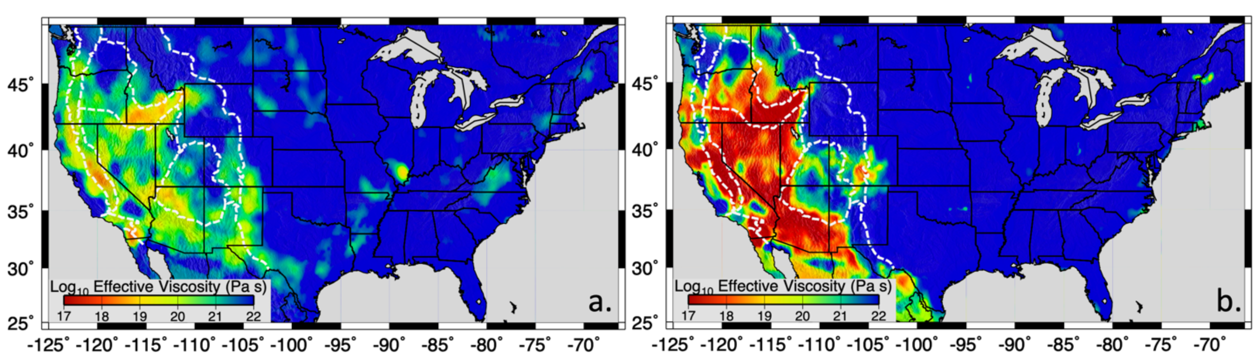

Figure 3. Effective viscosity at 60 km depth, with and without variable water fugacity. **a,** Effective viscosity attributable to temperature variations alone, imposing a constant (0.1% of saturation) water fugacity. **b,** Effective viscosity with water fugacity varied to match measured variations in lithospheric flexural rigidity.

2D and 3D Modeling of Simulated Earth Properties

This project's modeling component (co-PI Kanda) sought to address the role played by a rheologically strong and heterogeneous crust and lithosphere in modulating basal-lithospheric stressing rates from the asthenosphere/upper-mantle. Specifically, we want to investigate how basal mantle stress partitions into bending and membrane stresses under different assumptions for the rheological mechanisms (including linear vs. non-linear) and for the rheological and buoyancy properties. We hypothesized that modulation of deep flow stress forcing by lithospheric strength should manifest in crustal seismicity and surface geodetic strain-rate distributions. Predictions by these constrained models can also be compared to other near-surface observables including stress orientations and surface uplift rates. Given the large number of numerical, physical, and geometric parameters involved in self-consistent thermomechanical lithospheric dynamics models, especially in 3D, our modeling efforts began with detailed numerical/rheological sensitivity analysis to determine which factors most critically influence model predictions.

Benchmarking of ASPECT 2.0: After ensuring we had the necessary pre-requisite software versions, we compiled and installed ASPECT 2.0.0 on the two Utah-CHPC (UCHPC) nodes purchased via this grant. Initial tests applied the software to standard benchmark problems to verify that the code had compiled correctly, that it could solve the range of multiphysics it was designed for, and to assess the computational time required for particular types of simulations on a given number of processors. (The latter helps determine, for example, the minimum number of processors required for a particular rheology: e.g, highly non-linear rheologies require significant mesh refinement and thus more memory). We ran several benchmarks to test the validity of our installation on the UCHPC cluster. Fig. 4 presents results from an example benchmarking 2D linear viscous Stokes flow of a two-layer medium with an isoviscous lithosphere to assess how the adaptive mesh in ASPECT evolves as simulation progresses. For the (relatively) simple simulation shown, the number of finite-elements increased from ~16.5 thousand (~350 thousand degrees of freedom, DOF) at the initial time-step to 118.75 thousand (~2.5 million DOF) at the end of 20 Myr and required eight hours of computation. We did not see improvement beyond 32 processors (one whole node) for this problem, indicating that beyond this number of processors the communication latency between nodes prevents further gains in computational efficiency.

Tier-1 model tests: Following from analyses described earlier, we set up all modeling to incorporate a true free-surface that deforms in response to asthenospheric and lithospheric stress. We performed several numerical resolution tests to ascertain minimum cell sizes required to resolve relevant physical processes over the ~1 Myr time-scale of evolution for our "instantaneous" convection models. Since we are interested in 3D simulations, and our geophysical datasets have at best 20 km resolution, we initially explored simulations with coarse meshes (~5 km resolution). These models indicated that, using rheologies sensitive to temperature evolution, fixed-mesh solutions exhibit oscillatory and other unstable behavior over the time-scale of interest. With adaptive mesh refinement (AMR), solutions for these types of models evolve stably and in a physically realistic manner. We experimented with different AMR strategies (e.g., strain-rate, composition, temperature, density, or combinations thereof) and found that strain-rate and composition are two fundamental criteria, because any local changes in either can cause significant discontinuities in rheological strength. Next, we tested a suite of runs to investigate the surface response due to "instantaneous" (< 1 Myr) rising/sinking of anomalously dense or buoyant blobs ($\Delta\rho$ = ±0.3 to 0.6%) in the presence or absence of lithosphere and crust of varying viscous flow strengths. Fig. 5 illustrates examples of negatively buoyant blob sinking models. All of these simulations use AMR via the above strategy. The finest cells in these meshes typically occupy a small fraction of the model volume, but account for a large fraction of computational time.

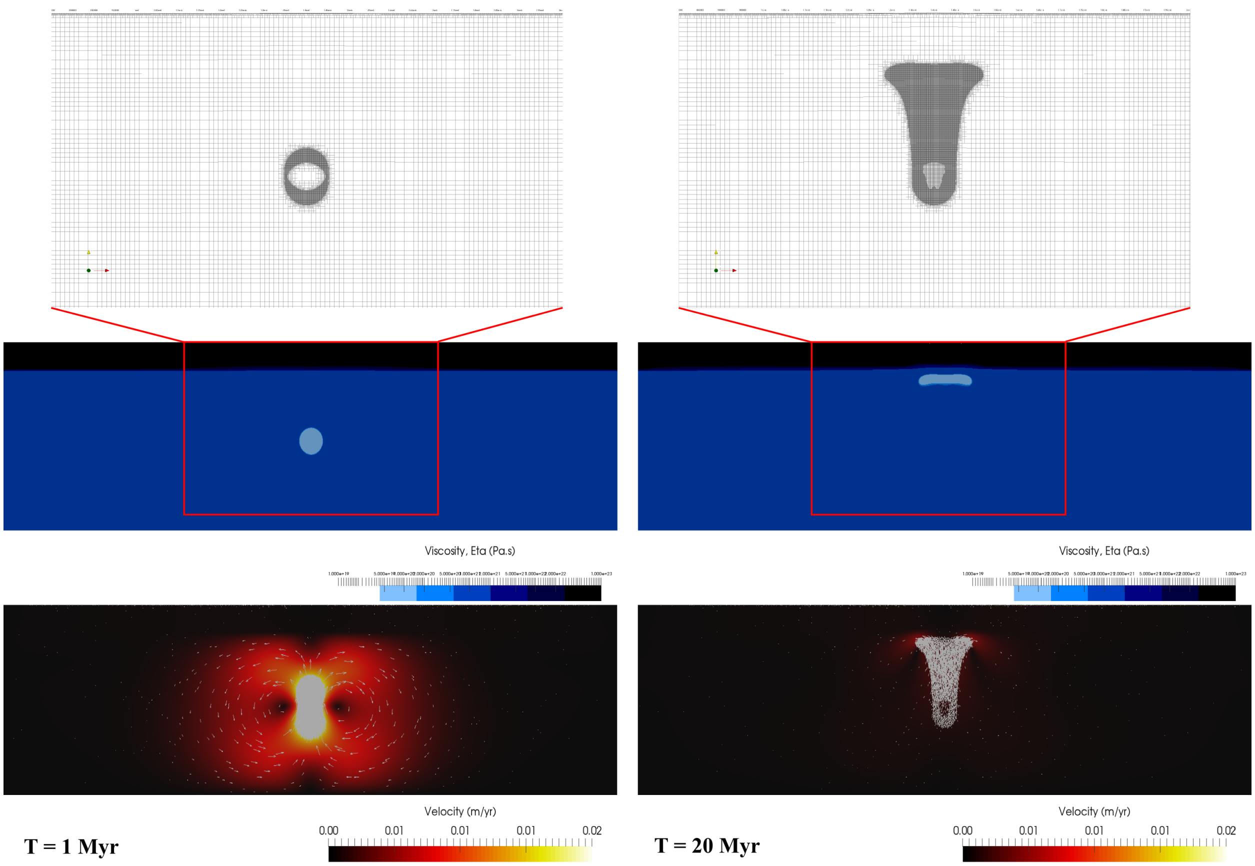

Figure 4. Linear viscous Stokes flow benchmark (assuming temperature-independent rheology). Evolution of the mesh (top), viscosity (middle), and flow field (bottom, white velocity vectors) at 1 Myr (left column, 44.7k elements) and 20 Myr (right column, 2.5M elements) after the start of simulation.

Significance of the rheological mechanism: Flow models with data assimilation typically use linear (diffusion creep) viscous rheologies that are independent of composition, and they usually assume state variables (e.g., strain-rate, temperature, and pressure) do not evolve during simulation. Becker et al. (2015), which motivated this research, relied on a linear viscous mechanical model with 1D isoviscous structure to infer basal-lithospheric stress rates, and other data-assimilation modeling studies (e.g., Moucha & Forte, 2011; Liu & Gurnis, 2010; Liu et al., 2010; Forte et al., 2010) also use linear viscosity (albeit with temperature- and pressure-dependence) while ignoring long-term strength of the lithosphere. Our modeling shows that the assumed mechanism of lithospheric and/or crustal flow significantly influences the magnitude and extent of free surface deflection, using four layered end-member models, including (Fig. 5a) two-layer linear isoviscous diffusion creep (with no temperature evolution); (Fig. 5b) two-layer diffusion creep in the mantle with an isoviscous lithosphere; (Fig. 5c) two-layer, T- and P-dependent diffusion creep in the mantle and lithosphere; and (Fig. 5d) four-layer composite diffusion-dislocation creep in addition to brittle-field plastic deformation in the uppermost lithosphere and crust. Models with an isoviscous lithosphere (Fig. 5ab) assume 10^{23} Pa s viscosity (as has been done in most previous data assimilation studies), two orders of magnitude more viscous than the ambient upper mantle. Viscosity exceeds 10^{25} Pa s in models where it is calculated at every step based on the relevant state variables (T, P), and for the composite case (d) with dependence on strain-rate and brittle plastic failure.

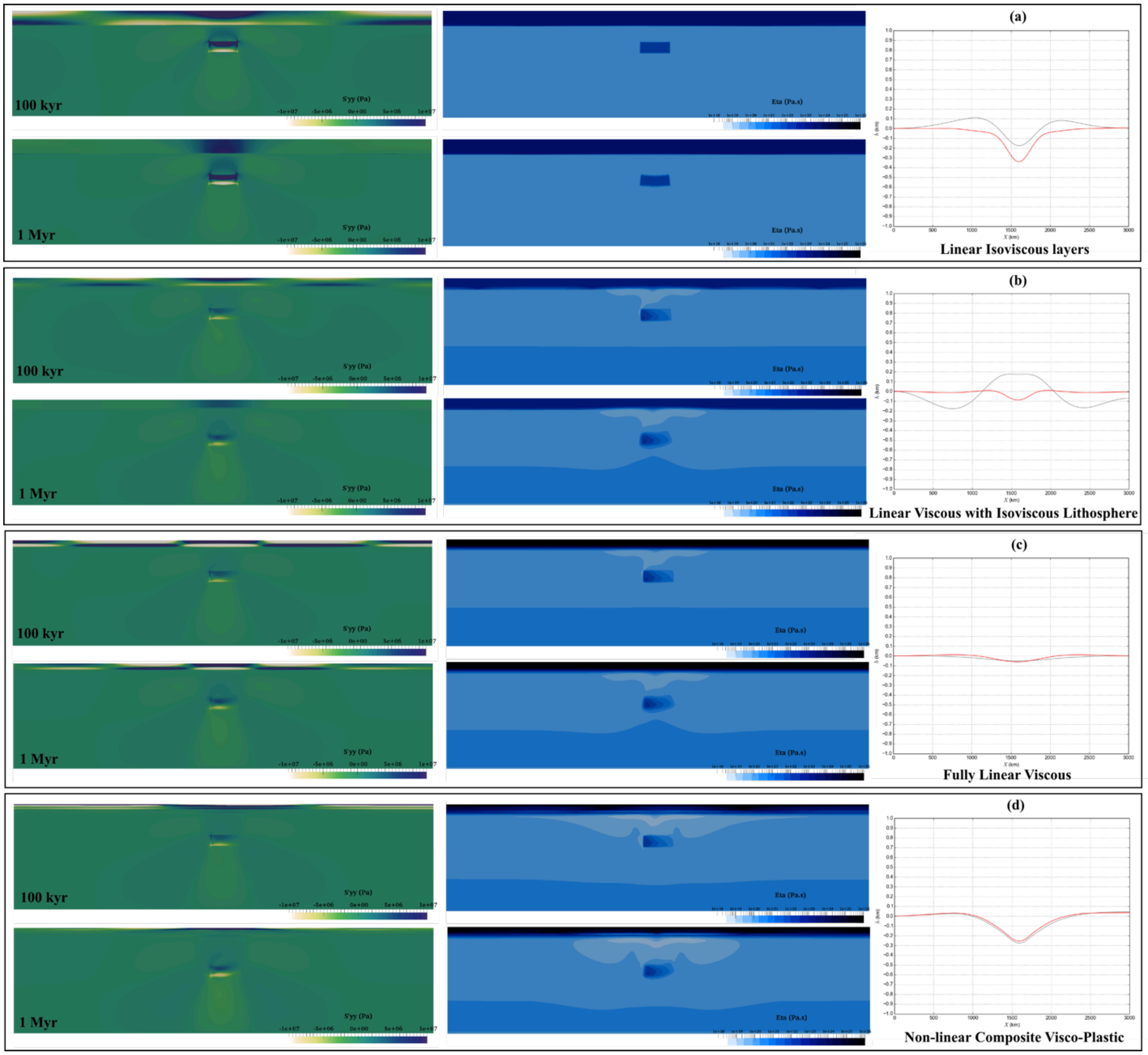

Figure 5. Vertical normal stress (left), viscosity (center) and free surface profile (right) at 100 kyr (grey) and 1 Myr (red) after start for different rheological parameterizations of the mantle, lithosphere, and crust. **a,** Linear iso-viscous (no temperature-, pressure-, or strain-rate dependence). **b,** Diffusion creep, with temperature- & pressure-dependence in the asthenospheric mantle but isoviscous (10^{23} Pa s) lithosphere. **c,** Diffusion creep in mantle and lithosphere, with temperature- & pressure-dependence. **d,** Composite diffusion plus dislocation creep and brittle-field plastic rheology.

The magnitude and pattern of stresses (and therefore strain-rates) induced in the lithosphere due to sinking of the cold blob are significantly different in all four models. Fig. 5 shows the deviatoric vertical normal stresses S'_{yy} (leftmost column), useful for comparing with surface deflection (rightmost column). Basal extensional stresses in the isoviscous (weaker) lithosphere models dissipate quickly (left column of Fig. 5ab). Fiber stress within the strong lithosphere resulting from *P*-*T*-dependent diffusion creep (left panel of Fig. 5c) is maintained even after 1 Myr of evolution. In contrast, initial stress contrasts in the upper/lower crust and lithosphere present in the more realistic composite rheology case are more focused at the surface right above the sinking blob because of the influence of strain-rate and localized plastic deformation on rheological strength (left panel of Fig. 5d). Thus, lithospheric/crustal strain-rate distribution, and hence the implications for seismicity, are significantly different for each of these models.

Clearly, the weaker lithosphere prescribed for isoviscous linear models results in surface deflection of shorter wavelength (Fig. 5ab) than their more realistic counterparts (Fig. 5cd). The topographic flexural bulge dissipates rapidly for a weak lithosphere (gray and red curves in Fig. 5ab) but is retained beyond 1 Myr for greater/more realistic lithospheric strengths (Fig. 5cd). Surface deflection of the most realistic composite rheology model (Fig. 5d) is more than twice that predicted by the purely diffusive counterpart (Fig. 5c). Thus, predicted surface uplift/subsidence rates and their patterns are significantly different under each of these model assumptions, and especially so over timescales of the order of 100 kyr or smaller.

Having established the optimal set of numerical (e.g., mesh resolution, extent and type of adaptive mesh refinement, domain boundary location) and structural parameters (e.g, four-layer models with composite rheology) that are necessary to optimally describe the dynamics, we can explore the dynamics of 2D and 3D models using the thermal and compositional buoyancy and rheology variations that were derived from physical state calculations applied to geophysical data above. We performed 2D cartesian tests with simulated-Earth properties in order to assess what resolution simulations can be realistically performed on our current two nodes (64-cores/256GB memory) at the Utah CHPC cluster. We developed a parallel python package (table2vtk) to convert the huge 3D datasets (temperature, density, viscosity prefactors) into structured grid datasets in the VTK format, to better visualize slices and cross-sections of the data along different transects. To assess how Aspect responds to the simulated-Earth fields, we input the inferred thermal structure into a 2D model of an E-W transect across the United States passing through Salt Lake City (Fig. 6). Incorporating density and viscosity pre-factors together into the models would require a modification of existing material models to treat each of the data sets as a compositional field, then re-compiling and benchmarking the updated code.

Discussion

Several significant results were discovered or strengthened in the course of performing these analyses. Among these:

• Initial exercises exploring various modeling assumptions by the undergraduate student, Jared Bryan, and CoPI Ravi Kanda illustrate that predictions of lithospheric stress and surface elevation are exceedingly sensitive to model accuracy in representing the free surface and the mechanism(s) of rheological laws. Presumably the rate-of-change of vertical normal stress examined by Becker et al. (2015) performed as well as it did as a predictor of seismicity because vertical normal stress is primarily sensitive to the vertical integral of buoyancy, but even vertical normal stress rates will be modulated lateral variations in the rheological properties of the medium. Consequently, we anticipate that improving on the predictive skill of the approach laid out in Becker et al. (2015)

will require both the model physics and the model material properties to simulate those of the real Earth as accurately as possible.

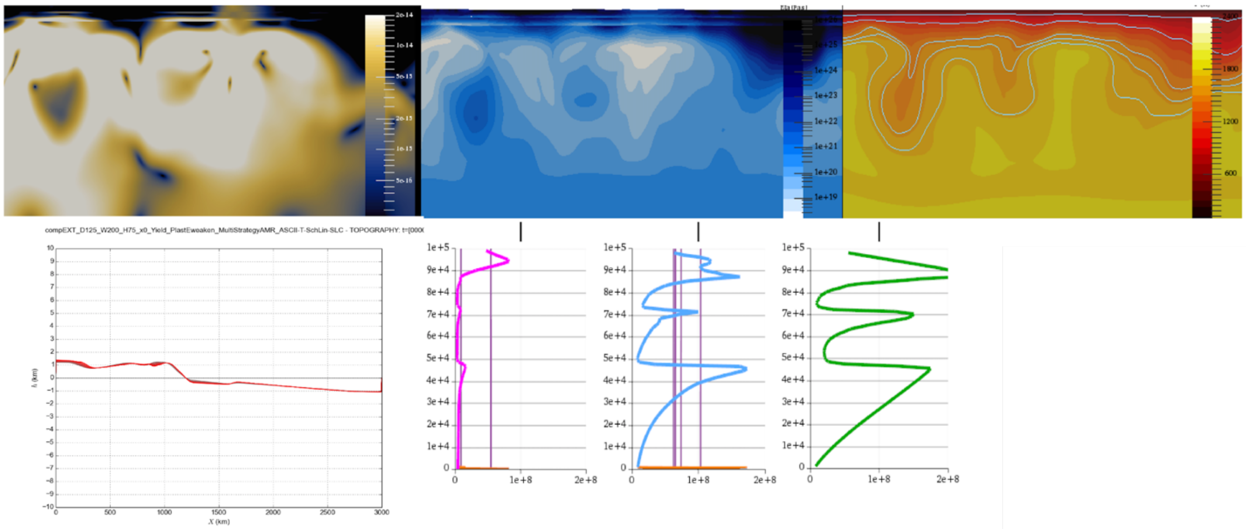

Figure 6. Model incorporating an E-W transect of estimated present-day thermal structure at the latitude of Salt Lake City, but with uniform crustal thickness, compositional density, and hydration state. Creep flow laws are nonlinear composite; brittle field is simulated by viscoplasticity. Top-left: strain rate (s^{-1}); top middle: viscosity (Pa s); top-right: temperature (°C); bottom left: topography (grey = 0.1 Myr; red = 1 Myr); bottom center: three profiles of differential stress in the lithosphere (upper 100 km of the model) near the right edge, center, and left edge of the transect.

• More realistic model physics and material properties that improve on the approach of Becker et al. (2015) will be necessary in any case, in order to extend the Molchan skill analysis approach to regions outside the western United States, because the background state of lithospheric stress and sign of the lithospheric stress rates require accurate book-keeping in order for a Molchan skill analysis of a prediction to succeed. For example, the Molchan skill analysis of geodetic strain rates in Becker et al. (2015) performed much better for shear strain rate (S = 0.28) than for dilatational strain rates (S = 0.16), despite the fact that strain in the Intermountain west is predominantly dilatational. Inspection shows that this is at least partly because geodetic dilatational strain is large and contractional in the northern Intermountain seismic belt (see their Extended Date Fig. 1e), despite the extensional expression of geologic structures and focal mechanisms in the region, and the negative sign of the strain rate penalizes the skill score of seismicity in that portion of the seismic belt as a consequence. (Indeed, the skill score would likely be much higher for dilatational geodetic strain rate if the absolute value were used.) A more recent study applying the Molchan skill analysis to rates of vertical normal stress in the central and southeastern U.S. (Saxena et al., 2021) and interpreted a negative skill score (S = –0.16) as a failure there. However, the negative sign likely reflects the fact that the tectonic environment there is transpressional rather than extensional (so a negative normal stressing rate will do more to augment the lithospheric state of stress toward failure. It is worth noting that S = –0.16 is likely still significant at three-sigma confidence (Becker et al., 2015), even if slightly less so than the S = 0.22 they calculated for gravitational potential energy. Nevertheless, predictive skill of geodynamical models are likely to greatly improve if the analyses can distinguish regions where dynamical forcing is driving lithospheric stress toward failure from those where it is driving it away, and that will require improved physics and characterization of material properties this project sought to address.

• Part of the effort during this project went toward improved characterization of the thermal model of the lithosphere through better conductive modeling of geotherms matching Pn-derived Moho temperature (Schutt et al., 2018) to surface heat flow (Blackwell et al., 2007). A discrepancy between Moho temperature and heat flow had previously been recognized by our group (Berry et al., 2014), but during the course of the project we carefully evaluated various hypotheses to explain the discrepancy including variations in mantle composition, variations in crustal thermal conductivity and radioactive heating parameterizations, and residual thermal perturbations from flat slab subduction (none of which are able to explain the discrepancy). The only remaining viable explanation is the heat absorbed by melting and released by hydration reactions in the context of metasomatism, and this interpretation appears to be supported by correlations of the thermal anomaly to elevation and to model predictions of elevation due to asthenospheric buoyancy and crustal compositional buoyancy. If correct, this has very far-reaching implications for the role of hydration enthalpy in dynamics, deformation and seismicity of subduction back-arc cordilleras the world over. The research will be submitted to Geology in the coming weeks (Berry et al., 2021 in prep).

• Careful analyses of mass buoyancy fields from lithospheric thermal, crustal thickness, crustal composition, and asthenospheric buoyancy fields (derived from seismic constraints for this project) indicate that many of these are strongly cross-correlated by the dynamical processes that generate mass density variations in the Earth (Lowry et al., 2019). This result implies that improved seismic constraints are absolutely crucial to teasing apart the depth-dependent sources of buoyancy that are responsible for topographic and gravity variations (which are insensitive to depth of mass but are often used to infer mass density structure). We are currently pursuing improved density modeling using Rayleigh-wave ellipticity and phase velocity measurements in collaboration with Fan-Chi Lin.

• Finally, modeling efforts for this project ran into limitations in the dynamical modeling code ASPECT that hampered full implementation of the seismically-derived simulated Earth fields in our models. However, conversations with the ASPECT developers led to submission of a collaborative proposal to NSF's Frontier Research in Earth Sciences program in 2019 to marry simulated Earth physical state fields like those developed for this grant with implementation of enhanced capabilities of ASPECT, in order to develop a modeling framework and realistic simulation of Earth properties to be shared with the Earth science community. That proposal was funded and efforts toward those goals are ongoing.

References

Becker, T.W., A.R. Lowry, C. Faccenna, B. Schmandt, A. Borsa & C. Yu (2015) Western U.S. intermountain seismicity caused by changes in upper mantle flow, *Nature*, *524*(7566), 458-461.

Berry, M.A., A.R. Lowry, D.L. Schutt, & R.V.S. Kanda (2014) Crustal geothermal properties and evidence of Laramide thermal perturbation of the western United States, AGU Fall Meeting, Abstr. T22B-04.

Blackwell, D.D., P.T. Negraru & M.C. Richards (2007) Assessment of the enhanced geothermal system resource base of the United States, *Nat. Resour. Res., 15*(4), 283–308.

Buehler, J.S. & P.M. Shearer (2017) Uppermost mantle seismic velocity structure beneath USArray, *J. Geophys. Res., 122*(1), 436-448.

Bürgmann, R. & G. Dresen (2008) Rheology of the lower crust and upper mantle: Evidence from rock mechanics, geodesy, and field observations, *Ann. Rev. Earth Planet. Sci., 36*.

Cammarano, F., S. Goes, P. Vacher & D. Giardini (2003) Inferring upper-mantle temperatures from seismic velocities, *Phys. Earth Planet. Inter., 138*(3–4), 197–222.

Christensen, N.I., & W.D. Mooney (1995) Seismic velocity structure and composition of the continental crust: A global view, *J. Geophys. Res., 100*(B6), 9761-9788.

Crameri, F., H. Schmeling, G. J. Golabek, T. Duretz, R. Orendt, S.J.H. Buiter, D.A. May, B.J.P. Kaus, T.V. Gerya & P.J. Tackley (2012) A comparison of numerical surface topography calculations in geodynamic modelling: an evaluation of the 'sticky air' method, *Geophys. J. Int., 189*(1), 38-54.

Forte, A.M., S. Quéré, R. Moucha, N.A. Simmons, S.P. Grand, J.X. Mitrovica & D.B. Rowley (2010) Joint seismic–geodynamic-mineral physical modelling of African geodynamics: A reconciliation of deep-mantle convection with surface geophysical constraints, *Earth Planet. Sci. Lett., 295*(3-4), 329-341.

Liu, L. & M. Gurnis (2010) Dynamic subsidence and uplift of the Colorado Plateau, *Geology, 38*(7), 663-666.

Liu, L., M. Gurnis, M. Seton, J. Saleeby, R. D. Müller, & J. M. Jackson (2010) The role of oceanic plateau subduction in the Laramide orogeny, *Nat. Geosci.*, *3*(5), 353-357.

Lowry, A.R. & M. Pérez-Gussinyé (2011) The role of crustal quartz in controlling Cordilleran deformation, *Nature, 471*(7338), 353-357.

Ma, X. & A.R. Lowry (2017) USArray imaging of continental crust in the conterminous United States, *Tectonics*, *36*(12), 2882-2902.

Molnar, P., P.C. England & C.H. Jones (2015) Mantle dynamics, isostasy, and the support of high terrain., *J. Geophys. Res., 120*(3), 1932-1957.

Montagner, J. P. & B.L.N. Kennett (1996) How to reconcile body-wave and normal-mode reference Earth models, *Geophys. J. Int., 125*(1), 229-248.

Moucha, R. & A.M. Forte (2011) Changes in African topography driven by mantle convection, *Nat. Geosci., 4*(10), 707-712.

Naliboff, J.B., S.J. Buiter, G. Péron-Pinvidic, P.T. Osmundsen, & J. Tetreault (2017) Complex fault interaction controls continental rifting, *Nat. Comm., 8*(1), 1-9.

Saxena, A., E. Choi, C.A. Powell & K.S. Aslam (2021) Seismicity in the central and southeastern United States due to upper mantle heterogeneities, *Geophys. J. Int., 225*(3), 1624-1636.

Schmandt, B. & F.C. Lin (2014) P and S wave tomography of the mantle beneath the United States, *Geophys. Res. Lett., 41*(18), 6342-6349.

Schutt, D.L., A.R. Lowry & J.S. Buehler (2018) Moho temperature and mobility of lower crust in the western United States, *Geology, 46*(3), 219-222.

Willett, S.D., D.S. Chapman & H.J. Neugebauer (1985) A thermo-mechanical model of continental lithosphere, *Nature, 314*(6011), 520-523.

• Project Data

Model fields from this research estimating physical state of the U.S., including 3D estimates of lithospheric and upper mantle asthenospheric temperature, density, effective viscosity, and constituent elements of dislocation creep rheology, are available from the PI upon request. The methods developed to create these fields currently are being improved and incorporated into the workflow for a new, global model simulating whole-Earth temperature, composition, density and rheology in collaboration with ASPECT model developers as part of an NSF Frontier Research in Earth Sciences project to create a solid-Earth science framework for Integrated Global Earth Models (NSF-FRES 1925575).

- **Bibliography of Publications and Presentations**

Berry, M.A., A.R. Lowry, X. Ma, R.V.S. Kanda & D.L. Schutt (2021) Cold, wet roots of high elevation in the western United States, *Geology*, in prep.

Bryan, J., A.R. Lowry & R.V.S. Kanda (2019) The role of flexural stresses in forecasting seismicity distributions, Utah Conference for Undergraduate Research (UCUR), Ogden UT.

Lowry, A.R., X. Ma, D.L. Schutt, M.A. Berry, J.S. Buehler & R.V.S. Kanda (2018) Evidence for hydration and its role in dynamics of the western U.S. Cordillera, Invited talk for the *2018 joint meeting of the CGU, CIG and ES-SSA*.

Lowry, A.R., R.V.S. Kanda, X. Ma, B. Scheppmann & D. Schutt (2018) Toward Earthquake System Science: In-situ physical state from geophysical properties, *AGU Fall Meeting*, T31H-0405.

Lowry, A.R., X. Ma, D.L. Schutt, R.V.S. Kanda & F.C. Lin (2019) Improving 3D density estimation with coupled seismic and gravity inversion, *AGU Fall Meeting*, S22C-08.

Lowry, A.R., D.L. Schutt & M. Pérez-Gussinyé (2021) Lithospheric strength and long-term stability express hydration and melt dynamics, *in prep*.

Kanda, R.V.S. (2018) Is flat subduction a consequence of rheologically strong lithosphere?, Invited talk for the *UC-Davis Department of Earth and Planetary Sciences Seminar Series*.

Kanda, R.V.S. & A.R. Lowry (2018) Towards Earthquake System Science: Constraining basal mantle stress partitioning within the lithosphere and crust, *AGU Fall Meeting*, T43G-0506.

Kanda, R.V.S., A.R. Lowry & S. Buiter (2021) Mounting wedge suction driven by lower mantle resistance triggers flattening of subducting slabs, *Geophys. Res. Lett.*, in prep.